Coastal Dynamics 2017
Paper No.262

ESTIMATING CLIMATE CHANGE IMPACTS ON STORM SURGE USING ADAPTIVE MESH REFINEMENT

Marc Kjerland[1], Nobuhito Mori[1]

Abstract

Coastal hazard assessment and mitigation requires a thorough understanding of extreme events such as severe storm surge. Limited observations and a changing climate pose an additional challenges for long-term planning and require ensemble modeling to be effective. Tropical cyclones (TCs) distributions are projected to change in a warming climate, but impacts to coastal communities require detailed simulations including local bathymetry features and often involve a wide range of spatial scales. Adaptive mesh refinement (AMR) is one approach to reduce computational costs by performing high-resolution simulation only in regions which require it, such as a coastal region experiencing storm surge, and minimizing costs elsewhere. To estimate the effects of climate change on extreme coastal hazards, we apply a dynamical downscaling methodology to generate two TC ensembles based on Typhoon Haiyan in 2013, one in the present climate and one in a pre-industrial climate. We then use these storm fields as forcing terms in GeoClaw, a storm surge model with AMR, to estimate the coastal impacts of these changes to TC distributions.

Key words: storm surge, climate change, numerical modeling, Typhoon Haiyan, adaptive mesh refinement, GeoClaw

1. Introduction

Storm surge, a coastal flooding hazard caused by tropical cyclones (TCs), is a major concern for coastal communities as highlighted by recent severe events such as Hurricane Sandy in 2012 and Typhoon Haiyan in 2013. For effective risk assessment and mitigation planning, accurate knowledge of extreme event distributions over long periods is desired. TC intensity has been observed to be increasing over the past few decades and is closely correlated with sea surface temperature (SST) rise (Emanuel, 2005). Climate change is projected to affect distributions of TCs including changes to storm tracks, frequency of cyclogenesis, and intensity (Mori and Takemi, 2016). However, estimation of the resulting impacts to coastal hazard distributions poses further challenges.

Storm surge is driven by strong winds and sea level pressure gradients but is highly sensitive to storm track and local bathymetry features which can amplify surge levels. As a result, careful understanding of TC behavior as well as ensemble modeling are necessary to make robust projections of surge events. However, since coastal inundation modeling occurs over a large range of spatial scales, with storm tracks extending thousands of kilometers and with human structures spanning tens of meters, numerical simulation can be challenging. To resolve the fine spatial scales along coastlines while minimizing total computation costs we implement a model with adaptive mesh refinement (AMR) that adjusts grid size dynamically to track features of interest. In this study we present a methodology to evaluate climate change impacts on storm surge events using this lower computational approach.

In November 2013 the coastal city of Tacloban in the Philippines was devastated by Typhoon Haiyan, one of the most intense TCs to make landfall ever recorded. Tacloban experienced storm surge of over 5m and the region suffered nearly 6000 casualties. Assessment of such worst-case extreme weather events is important for disaster prevention and mitigation. However, estimating the severity of future events is difficult with limited historical observations and a changing climate. To assess the potential impact of climate change on extreme events such as this one, an approach known as probabilistic event attribution has been proposed (Pall *et al*, 2011). Under this framework, two sets of ensemble simulations are performed using an atmospheric general circulation model (AGCM) - one which includes the effects of anthropogenic greenhouse gas forcing and one which does not. In this study we investigate changes in severity for the Haiyan surge event based on observed climate conditions and on a projected pre-industrial

climate condition. Since SST and air temperature are the important climatic factors for TC intensity (Emanuel, 2005) we incorporate their change in our approach. It should be noted that in this study we are only interested here in the potential amplification of a worst-case event and not in its frequency.

In this study we use ensemble dynamical downscaling from a 60 km AGCM to a high-resolution 1 km mesoscale forecast model to reproduce the TC Haiyan event, considering both present-day and pre-industrial climate conditions. Then we use the resulting wind and pressure fields as momentum forcing terms in a depth-averaged ocean model to generate storm surge in the target location at Leyte Gulf. Finally we compare the surge levels between the two ensembles and estimate the contribution of climate change to the severity of the TC Haiyan surge event.

2. Methodology

To produce the tropical cyclone ensembles (whose wind and pressure fields will be used as forcing terms in the storm surge model) we follow the dynamical downscaling methodology of Takayabu *et al*, (2015) but where those authors used SuWAT for their surge model we use GeoClaw. A schematic diagram of the downscaling methodology is shown in Figure 1. The parent model, used to obtain the initial and boundary conditions, is the Japan Meteorological Agency's Weekly Ensemble Prediction (WEP) model (Sakai *et al,* 2009). The WEP is a global spectral model with an effective 60 km resolution and an ensemble of 51 members was produced using the singular vector method (Buizza and Palmer, 1995). Downscaling to 1-km resolution was then performed using a series of nested models to avoid producing shocks at the boundary. First was a non-hydrostatic regional climate model (NHRCM) (Sasaki *et al*, 2011) at 20 km resolution, where spectral nudging was applied to reproduce the TC track of the parent model. The next step was using the NHRCM at 5 km resolution (NHRCM05) with a Kain-Fritsch convective parametrization scheme (Kain and Frisch, 1990, 1993). Storm tracks computed by NHRCM05 are shown in Figure 2. Then a high-resolution Weather Research and Forecasting (WRF) model was used incorporating explicit cloud microphysics (Skamarock *et al*, 2008), first at 3-km and finally at 1-km resolution.

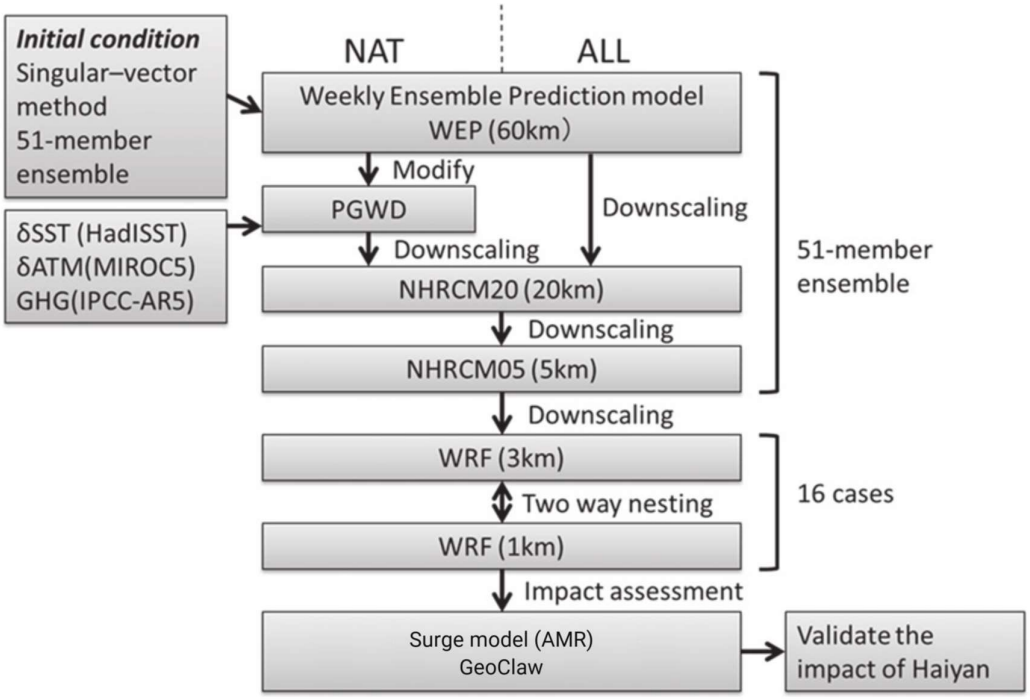

Figure 1. Schematic diagram of PGWD methodology (adapted from Takayabu *et al*, 2015).

In the previous study of Takayabu *et al* (2015), due to computational constraints only a subset of the

ensemble members was used in the WRF downscaling. For comparison with this study we use a similar subset determined as follows. First, to capture the range of TC behavior in the ensemble, three cases were selected: case 02m whose track passed closed to the observed track at Samar and Leyte Islands (roughly at 11N° 125E°); case 11m which had the lowest minimum central pressure (MCP) in NHRCM05; and case 18p which had the highest MCP in NHRCM05. Then, to capture the storm surge levels around Tacloban, all ensemble members whose storm track passed within 50 km of the observed track at Samar and Leyte Islands were selected. Seven additional members met this criteria: cases 05m, 12m, 15m, 21m, 25m, 06p, and 09p. Initial integration time for all cases was set at 18UTC 5 November 2013 (referred to as #1001). For case 02m, two additional integration times were considered: 12UTC 5 November (#1000) and 00UTC 6 November (#1002). In total twelve ensemble members were considered for the WRF downscaling and storm surge simulation.

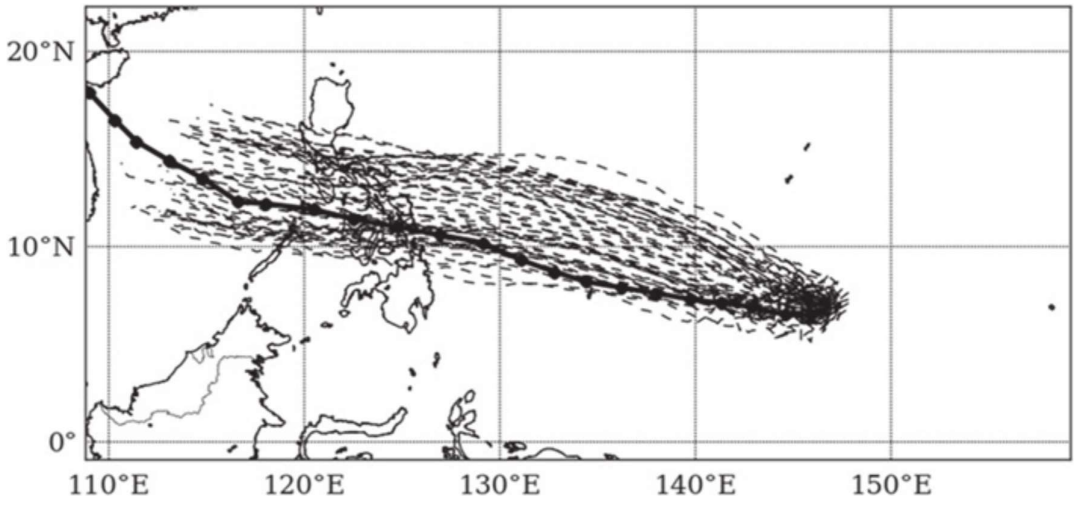

Figure 2. Storm tracks of Typhoon Haiyan ensemble computed by NHRCM05. The solid black line represents best track data marked at six-hour intervals (from Takayabu *et al,* 2015).

A pre-industrial climate ensemble (denoted NAT) is generated from the present-day climate ensemble (denoted ALL) using the Pseudo Global Warming Downscaling (PGWD) methodology, where differences in SST and air temperature between past and present climates are incorporated in the boundary conditions when downscaling from WEP. The anthropogenic SST warming is derived from the linear trend in monthly data from Hadley Centre Sea Ice and Sea Surface Temperature data set for 1870-2012 (Rayner *et al,* 2003, Christidis and Stott 2014, Shiogama *et al*, 2014), with a difference ranging from 0.2 K to 0.8 K in the target area (100°-180°E, 5°-25°N). The air temperature warming is derived from two ensemble simulations of the MIROC5-AGCM (Watanabe *et al,* 2010, Shiogama *et al,* 2014) using the SST signal. The average tropospheric and stratospheric differences in the target area in November of 2010-2012 were +0.5K and -1.5K, respectively. For more details see Takayabu *et al* (2015).

3. Numerical storm surge model

In this study we model the long-wave behavior of storm surge including inundation over land. We do not consider the effect of waves and tides, and although these can be significant the maximum tidal range in the target area is 0.7 m and was close to mean water level when Haiyan made landfall.

The governing equations for the surge model are the nonlinear shallow water equations with bathymetry and source terms:

$$\begin{aligned}
\frac{\partial}{\partial t}h + \frac{\partial}{\partial x}(hu) + \frac{\partial}{\partial y}(hv) &= 0 \\
\frac{\partial}{\partial t}(hu) + \frac{\partial}{\partial x}\left(hu^2 + \frac{1}{2}gh^2\right) + \frac{\partial}{\partial y}(huv) &= -gh\frac{\partial b}{\partial x} + S_x \\
\frac{\partial}{\partial t}(hv) + \frac{\partial}{\partial x}(huv) + \frac{\partial}{\partial y}\left(hv^2 + \frac{1}{2}gh^2\right) &= -gh\frac{\partial b}{\partial y} + S_y
\end{aligned}$$

where h is water column height, u and v are depth-averaged velocities, g is the gravitational constant, and b is bathymetry height. The remaining source terms S_x and S_y are given by:

$$\begin{aligned}
S_x &= fhv + \frac{h}{\rho}\left(\frac{-\partial P_a}{\partial x} + \rho_{air}C_w|\vec{W}|W_x - C_f|\vec{u}|u\right) \\
S_y &= -fhu + \frac{h}{\rho}\left(\frac{-\partial P_a}{\partial y} + \rho_{air}C_w|\vec{W}|W_y - C_f|\vec{u}|v\right)
\end{aligned}$$

where f is the Coriolis parameter, ρ and ρ_{air} are densities of water and air, P_a is sea level pressure, C_w and C_f are the wind stress and bottom friction coefficients, and $W=(W_x, W_y)$ is wind speed.

The bottom friction is given by a Manning's n law:

$$C_f = gn^2h^{-1/3}$$

where $n=0.022$ for regions below mean sea level and $n=0.03$ for regions above mean sea level.

The wind stress coefficient is given by a Mitsuyasu & Kusaba law:

$$C_w = \begin{cases} \left(1.290 - 0.024|\vec{W}|\right) \times 10^{-3}, & if|\vec{W}| < 8 \\ \left(0.581 + 0.063|\vec{W}|\right) \times 10^{-3}, & if|\vec{W}| \geqslant 8 \end{cases}$$

This wind drag coefficient is typically used with an upper bound at 30 m/s. However, since our surge model doesn't incorporate short wave effects we compensate by omitting the upper limit, as suggested by (Kawai, et al, 2011).

For the numerical storm surge model we use GeoClaw, a finite volume solver for 2-dimensional (depth-averaged) flows with AMR (Mandli *et al* 2016, Mandli and Dawson, 2014, Clawpack Development Team, 2017) . GeoClaw employs Riemann solvers for numerical evolution including shocks and inundation conditions. Radiative boundary conditions are used at lateral boundaries. The domain is spatially discretized by logically-rectangular grids of size 0.25°, with variable grid resolution determined at runtime based on state variables and forcing terms. A total of six refinement levels were used, with grid refinement ratios of 1:2 from levels 1 to 5 and 1:4 at level 6 (corresponding to a grid size of roughly 400 m). Grid refinement is based on water current speed (refinement at intervals of 1 m/s), water height from sea level (full refinement at 1 m deviation), wind speed (refinement at 20 m/s, 40 m/s, 60 m/s), and proximity to the storm center (refinement at 60 km, 40 km, 20 km). A snapshot of wind speeds and refinement regions is shown in Figure 3.

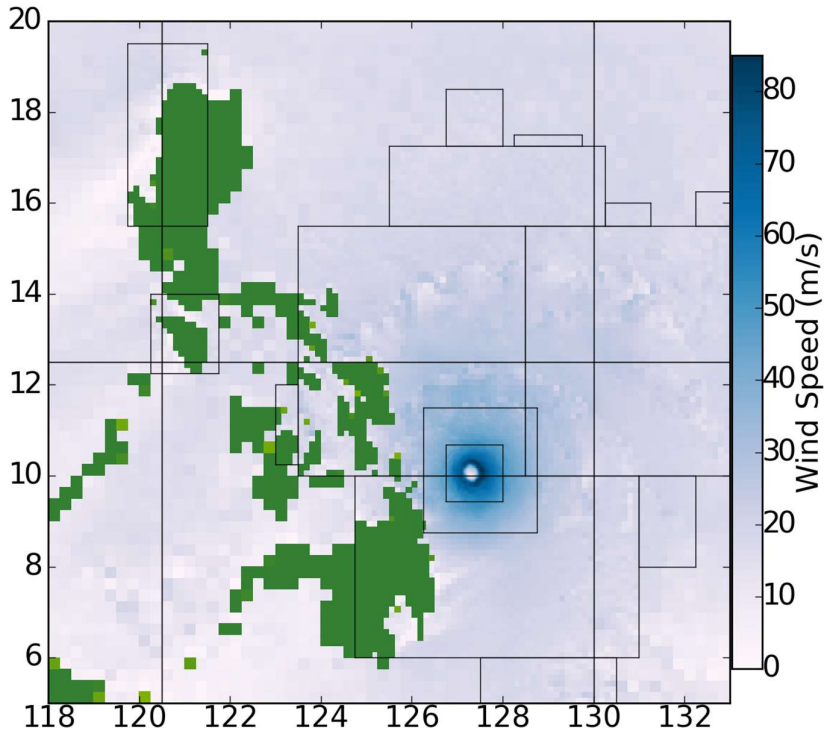

Figure 3. Snapshot of wind speeds for a Haiyan-like storm. Black rectangles indicate regions of grid refinement in GeoClaw surge model, based on proximity to storm center, wind speed, and water current speed.

The computational domain is the region 111°E to 149°E and from 4°S to 29°N. Elevation data is provided by the General Bathymetric Chart of the Oceans GEBCO 2014 Grid (GEBCO, 2014) with resolution of 30 arc-seconds (roughly 1km). Atmospheric forcing terms are given by the corresponding WRF 1 km simulation data at 1-hour intervals. Forcing data at other times is given by estimating the storm center via linear interpolation of the storm centers in the preceding and following storm snapshots, followed by shifting the two snapshots accordingly and applying a weighted average. Landfall times are different for each member, but integration begins roughly two days before landfall and ends roughly two days after landfall. Timestep size in each refinement region is determined based on the CLF condition.

4. Results and discussion

Mininum central pressure ranged from 951 hPa to 906 hPa (compared with actual estimated minimum central pressure of 895 hPa) and maximum wind speeds ranged from 50 m/s to 63 m/s (compared with actual estimated wind speed of 64 m/s). Comparing the NAT and ALL ensembles, there was an average increase in intensity of 6.6 hPa and 3.2 m/s in the present climate with a significance level of 1% (Takayabu *et al*, 2015). A comparison of these typhoon characteristics is shown in Figure 4.

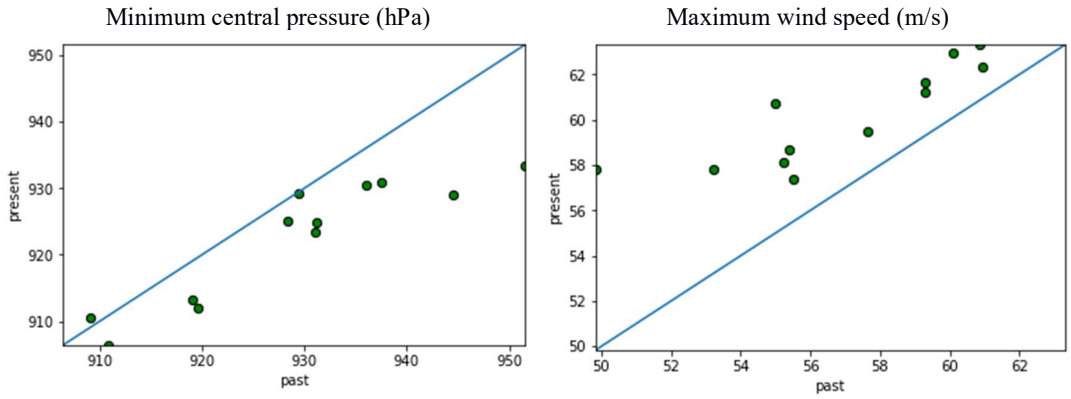

Figure 4. Comparison of minimum central pressure (left) and maximum wind speed (right) between corresponding ensemble members of past and present climate scenarios.

Maximum surge level is given as maximum water height about mean sea level in the Leyte Gulf area, from 124.9°E to 125.9°E and from 10.4°N to 11.4°N, monitored at a spatial resolution of approximately 1 km in space and 10 minutes in time. Maximum surge ranged from 0 m (case #1001 11m NAT) to 3.9 m (case #1001 02m NAT). Mean maximum surge level was 1.70 m in the NAT ensemble and 2.04 m in the ALL ensemble, suggesting an increase of 20% in surge height. Standard deviations were 1.29 m and 1.20 m, respectively. A summary of the numerical results is shown in Table 1.

Case name	MCP (hPa)	Max wind speed (m/s)	Max surge height (m)	Runtime (s)
NAT #1000 02m	919.12	60.93	2.86	1122
ALL #1000 02m	913.26	62.34	1.71	1036
NAT #1001 02m	910.86	60.10	3.86	1240
ALL #1001 02m	906.46	62.96	2.32	1094
NAT #1002 02m	909.12	60.84	3.57	1276
ALL #1002 02m	910.65	63.31	1.62	1259
NAT #1001 05m	928.42	59.29	1.44	905
ALL #1001 05m	925.09	61.63	2.19	1011
NAT #1001 06p	929.49	55.51	1.84	884
ALL #1001 06p	929.28	57.36	2.67	893
NAT #1001 09p	931.24	55.38	2.64	1086
ALL #1001 09p	924.91	58.68	2.00	1009
NAT #1001 11m	919.64	53.20	0.40	860
ALL #1001 11m	911.93	57.84	3.59	2316
NAT #1001 12m	931.06	57.64	0.84	868
ALL #1001 12m	923.46	59.47	3.63	1081
NAT #1001 15m	936.06	55.22	0.39	1383
ALL #1001 15m	930.37	58.14	0.26	1659
NAT #1001 18p	937.47	59.30	0.86	941
ALL #1001 18p	930.8	61.19	1.05	969
NAT #1001 21m	951.54	49.83	0.00	666
ALL #1001 21m	933.42	57.82	0.06	1012
NAT #1001 25m	944.51	54.99	1.70	1086
ALL #1001 25m	929.12	60.70	3.47	1875

Table 1. Summary of ensemble member experiments. Mean central pressure (MCP) and maximum wind speed are from the entire computation, but the maximum surge height is observed only in the target region

around Leyte Gulf. Runtime is wall time using 32 threads.

Maximum water levels at Leyte Gulf for each ensemble member are shown in Figure 5 for the present-day ensemble and in Figure 6 for the pre-industrial ensemble. Note that maximum water level monitoring here is performed only at regions of grid refinement level 3 and above, so some cases with low surge levels appear to have blocky regions of higher water levels.

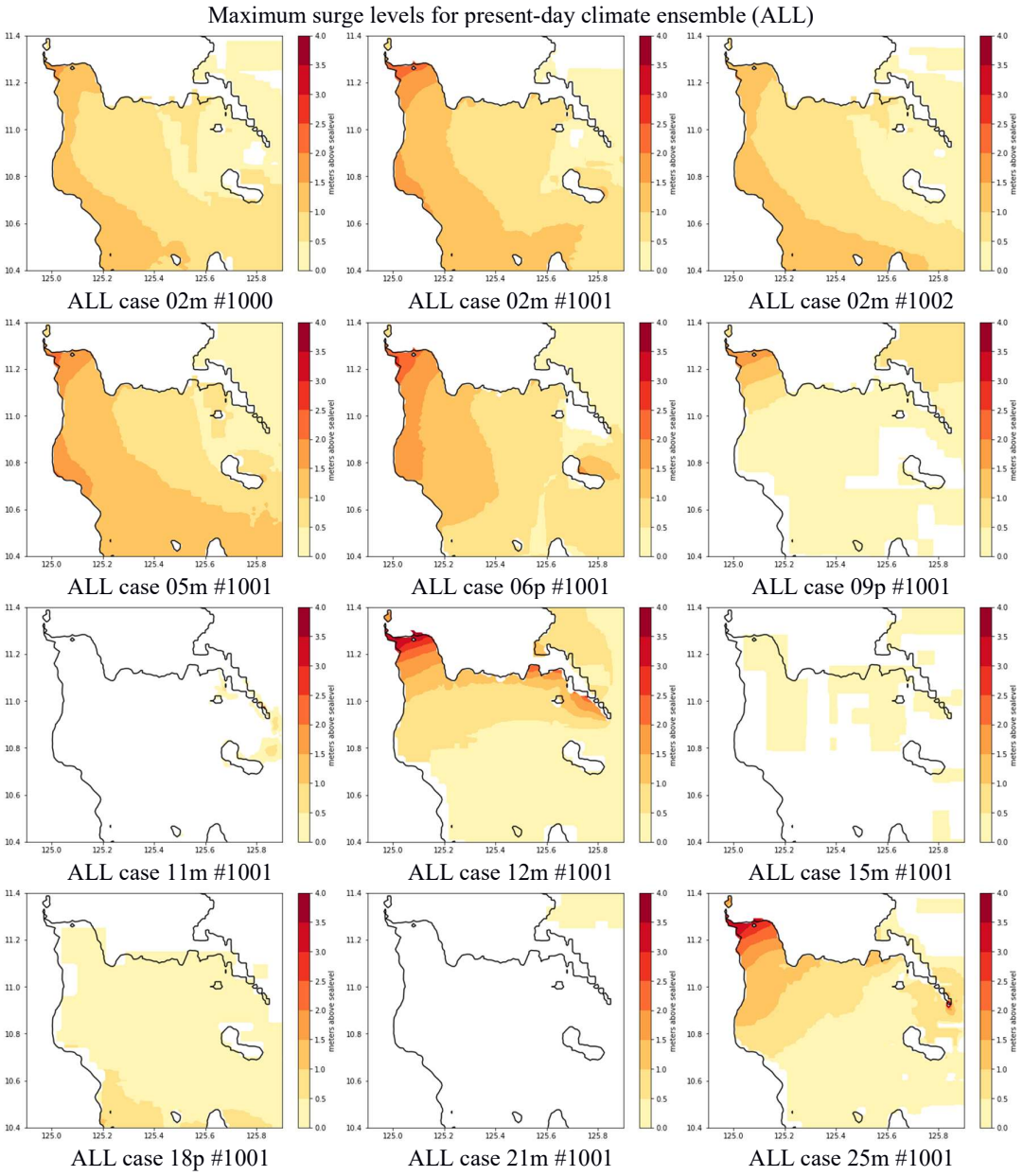

Figure 5. Maximum water level at Leyte Gulf for ensemble members in the present-day ensemble (ALL). The color range is from 0 to 4 m.

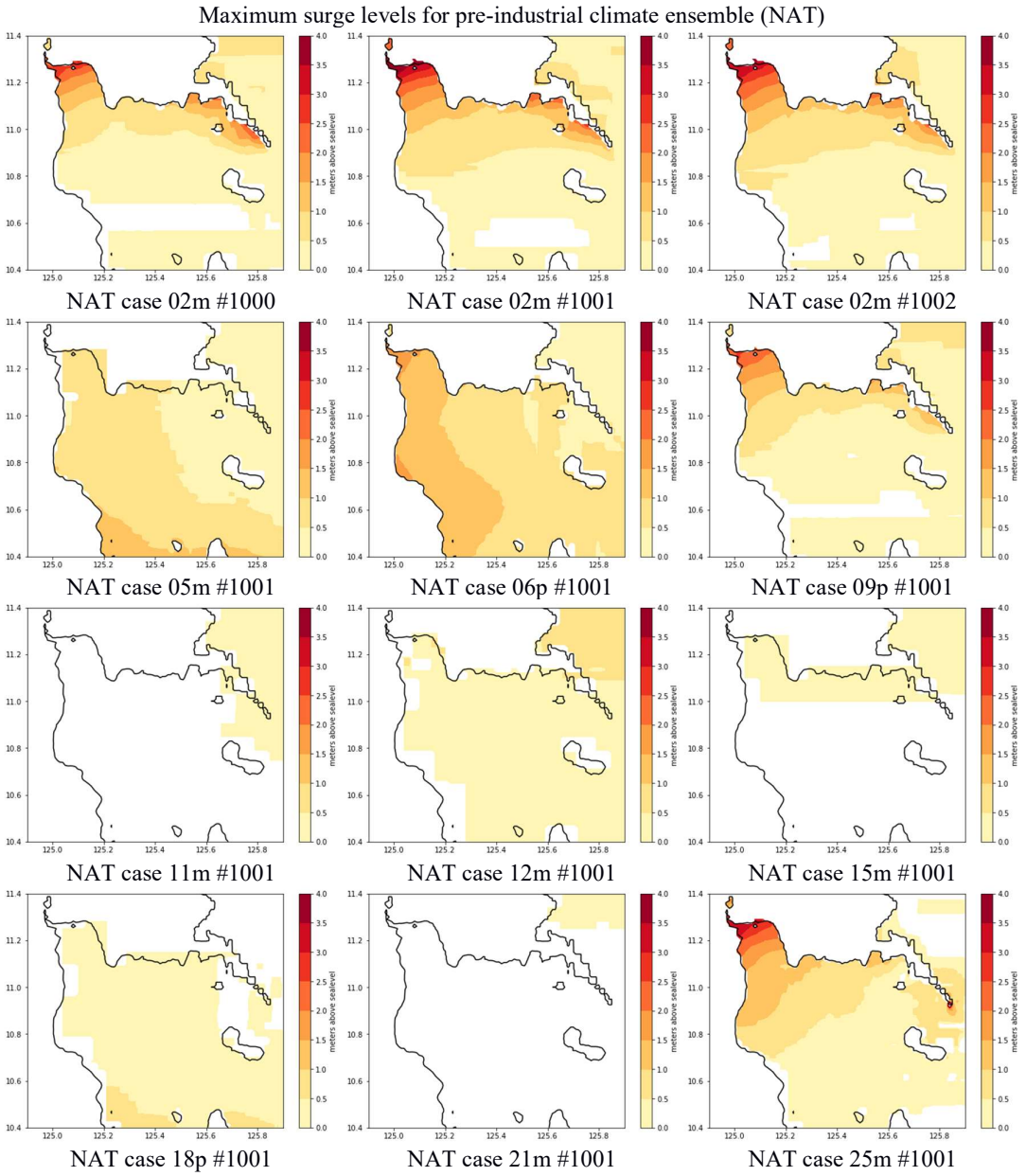

Figure 5. Maximum water level at Leyte Gulf for ensemble members in the present-day ensemble (ALL). The color range is from 0 to 4 m.

We see from Figures 5 and 6 a striking variety of surge distributions. Storm track was a very important factor in determining surge height in this experiment, especially due to the amplification effects of geographic features at Leyte Gulf (Mori *et al* 2014). Despite increased intensity in all storms in the present climate compared with past climate, surge height did not uniformly increase and in several cases actually decreased. In terms of TC modeling, a storm track deviation on the order of tens of kilometers is fairly low but can result in drastically different surge estimates.

Using AMR allows for greatly reduced computation time. Each of these simulated 4-day scenarios, with spatial resolution as high as 400m, took 10-40 minutes of wall time using 32 threads. While conventional fixed nested grids can also be efficient, the computation cost with AMR depends on the

severity of the storm surge so in ensemble modeling most runs will have lower cost than the worst-case scenario. In this experiment, only three runs out of twenty-four required more than 25 minutes of computation.

5. Conclusions

Estimation of extreme coastal hazards considering the influence of climate change is an important but challenging problem for hazard estimation and mitigation. In this study a dynamical downscaling ensemble framework has been presented to estimate the effect of climate change on an extreme storm surge event in the Philippines. It is indicated that surge levels for a Typhoon Haiyan-like storm would have been roughly 20% lower in a pre-industrial climate, based on atmospheric downscaling experiments incorporating projected climate trends. However, due to the large effect of geographical features in amplifying surge height and the wide range of storm tracks in the TC ensemble, it is difficult to be certain of this projected result without a larger ensemble.

Low cost models are vital to performing efficient ensemble projections for coastal inundation and AMR methods provide a useful and effective tool for these projections. The cost of computing storm surge in such dynamical downscaling experiments can now be considered minimal, so possibly low-cost atmospheric models should be considered for larger ensembles. In particular, since surge height is so sensitive to storm track it is especially important to use a large ensemble of tropical cyclones for more robust trend estimation. Further studies could incorporate the frequency of tropical cyclones under climate change with storm track and intensity to provide more usable estimates of extreme event distributions for hazard mitigation.

References

Buizza, R. and Palmer, T., 1995. The singular-vector structure of the atmospheric global circulation. *Journal of the Atmospheric Sciences*, 52(9):1434–1456.

Christidis, N. and Stott, P. A., 2014. Change in the odds of warm years and seasons due to anthropogenic influence on the climate. *Journal of Climate*, 27(7):2607–2621.

Clawpack Development Team, 2017. Clawpack software. Version 5.4.0.

Emanuel, K., 2005. Increasing destructiveness of tropical cyclones over the past 30 years. *Nature*, 436(7051):686–688.

Fritsch, J. M. and Kain, J. S., 1993. Convective parameterization for mesoscale models: the Fritsch-Chappell scheme. *The Representation of Cumulus Convection in Numerical Models*, pages 159–164. Springer.

General Bathymetric Chart of the Oceans, 2015. The GEBCO 2014 Grid. Version 20150318, data retrieved from www.gebco.net.

Kain, J. S. and Fritsch, J. M., 1990. A one-dimensional entraining/detraining plume model and its application in convective parameterization. *Journal of the Atmospheric Sciences*, 47(23):2784–2802.

Kawai, H., Hashimoto, N., Yamashiro, M., and Yasuda, T., 2011. Uncertainty of extreme storm surge estimation by high wind sea surface drag coefficient and future typhoon change. *Coastal Engineering Proceedings*, 1(32):18.

Mandli, K. T., Ahmadia, A. J., Berger, M., Calhoun, D., George, D. L., Hadjimichael, Y., Ketcheson, D. I., Lemoine, G. I., and LeVeque, R. J., 2016. *Clawpack: building an open source ecosystem for solving hyperbolic PDEs*. PeerJ Computer Science, 2:e68.

Mandli, K. T. and Dawson, C. N., 2014. Adaptive mesh refinement for storm surge. *Ocean Modelling*, 75:36–50.

Mori, N., Kato, M., Kim, S., Mase, H., Shibutani, Y., Takemi, T., Tsuboki, K., and Yasuda, T., 2014. Local amplification of storm surge by super typhoon Haiyan in Leyte Gulf. *Geophysical Research Letters*, 41(14):5106–5113.

Mori, N. and Takemi, T., 2016. Impact assessment of coastal hazards due to future changes of tropical cyclones in the north Pacific Ocean. *Weather and Climate Extremes*, 11:53–69.

Pall, P., Aina, T., Stone, D. A., Stott, P. A., Nozawa, T., Hilberts, A. G., Lohmann, D., and Allen, M. R., 2011. Anthropogenic greenhouse gas contribution to flood risk in England and Wales in Autumn 2000. *Nature*, 470(7334):382–385.

Rayner, N., Parker, D. E., Horton, E., Folland, C., Alexander, L., Rowell, D., Kent, E., and Kaplan, A., 2003. Global analyses of sea surface temperature, sea ice, and night marine air temperature since the late Nineteenth Century. *Journal of Geophysical Research: Atmospheres*, 108(D14).

Sasaki, H., Murata, A., Hanafusa, M., Oh'izumi, M., and Kurihara, K., 2011. Reproducibility of present climate in a non-hydrostatic regional climate model nested within an atmosphere general circulation model. *SOLA*, 7:173–176.

Shiogama, H., Watanabe, M., Imada, Y., Mori, M., Kamae, Y., Ishii, M., and Kimoto, M., 2014. Attribution of the

June-July 2013 heat wave in the Southwestern United States. *SOLA*, 10:122–126.

Takayabu, I., Hibino, K., Sasaki, H., Shiogama, H., Mori, N., Shibutani, Y., and Takemi, T., 2015. Climate change effects on the worst-case storm surge: a case study of typhoon Haiyan. *Environmental Research Letters*, 10(6):064011.

Watanabe, M., Suzuki, T., Oishi, R., Komuro, Y., Watanabe, S., Emori, S., Takemura, T., Chikira, M., Ogura, T., Sekiguchi, M., et al., 2010. Improved climate simulation by MIROC5: mean states, variability, and climate sensitivity. *Journal of Climate*, 23(23):6312–6335.

William, C. S., Joseph, B., Jimy, D., David, O., Dale, M., Michael, G., Huang, X., Wang, W., and Jordan, G., 2008. A description of the Advanced Research WRF version 3. *NCAR Technical Note*, 126.

Yamaguchi, M., Sakai, R., Kyoda, M., Komori, T., and Kadowaki, T., 2009. Typhoon ensemble prediction system developed at the Japan Meteorological Agency. *Monthly Weather Review*, 137(8):2592–2604.